

The synthesis of ultrafine titanium nitride in an r.f. plasma

TOYONOBU YOSHIDA, AKIHISA KAWASAKI, KUNIHICO NAKAGAWA, KAZUO AKASHI

Department of Metallurgy and Materials Science, Faculty of Engineering, The University of Tokyo, Bunkyo-ku, Tokyo, 113, Japan

The ultrafine titanium nitride particles with a statistical median size of about 10 nm were prepared by passing pure titanium powder ($< 25 \mu\text{m}$) through a radio-frequency (r.f.) argon–nitrogen plasma. The effects of the $[\text{N}_2]/[\text{Ti}]$ molar ratio of the reactant on the nature of the products were investigated by chemical analysis, X-ray diffraction and electron microscopy. The conversion efficiency was close to 100%. The colour of the product was black, which is attributed to the particle size ranging from 5 to 150 nm. Most of the crystallites were single crystal and showed clear-cut habits of cubic phase. The chemical composition and lattice parameter of the products changed with the $[\text{N}_2]/[\text{Ti}]$ ratio. The thermodynamics of the process were also considered. These results provide evidence to suggest that new materials can be produced by an r.f. plasma process, in particular, the ultrafine refractory nitrides.

1. Introduction

There has been increasing interest in the possibilities of an r.f. plasma for several fields of application. The most promising field would be in the chemical synthesis of ultrafine refractory materials, such as carbides and nitrides, although the studies in this field are in an early stage. If clean and uniform ultrafine powders can easily be prepared by the r.f. plasma process, there will be a rapid development in many specialized fields of application [1]. The most important application will be in the field of powder metallurgy, because of their high sinterability [2, 3].

Several reactions for the synthesis of refractory materials in r.f. plasmas were reviewed by Waldie [4] and Mahe [5]. One possible process is the reaction between metal halides and reactive gases, which have been widely used in ordinary chemical-vapour deposition. Recently, Troitskii *et al.* [6] studied the preparation of titanium nitride and titanium boronitrides in an r.f. nitrogen–hydrogen plasma. Mackinnon *et al.* [7] also used this process developing the method of the synthesis of ultrafine boron carbide successfully. Their results showed that the composition of the products can

be controlled linearly with that of reactants. With this method, however, post-treatment is needed to remove by-products, such as HCl, NH_4Cl and imides, which may be formed in the process simultaneously.

Another possible process is a more direct one in which pure metallic powders are used as starting materials. Under the appropriate conditions, the metallic powders are vaporized completely in a plasma region and react directly with reactive gases. The advantages of this process are its simplicity, flexibility, and that the above-mentioned by-products can be minimized. By this method, Canteloup and Mocellin [8] recently tried to synthesize ultrafine nitrides. They showed that ultrafine aluminium and silicon nitrides could be obtained starting from $35 \mu\text{m}$ aluminium and silicon powders, and ammonia gas as nitriding agent, although the impurity oxygen content in their products was fairly high. In their experiments, the reactants were introduced into the tail flame. When nitrogen gas was used as nitriding agent, all attempts were largely unsuccessful because of the low conversion rate.

If possible, however, nitrogen gas is more

desirable as nitriding agent because by-products such as imides would not be formed during the reaction. In this study, the synthesis of ultrafine titanium nitride was attempted by introducing titanium powder into an argon-nitrogen plasma. A reactor chamber was designed for this study and the products were investigated with emphasis on a correlation between $[N_2]/[Ti]$ molar ratio and the composition of the products. The morphology of the particles was also investigated.

2. Thermodynamic considerations

Thermodynamic equilibrium compositions for the Ti–N₂–Ar system were calculated up to a temperature of 6000 K which is supposed to be consistent with the plasma flame temperature immediately below a coil region of an r.f. plasma torch. The chemical species considered in this calculation are nine gaseous species (Ar, Ar⁺, Ti(g), Ti⁺, N₂, N, N⁺, e⁻, TiN(g)) and two condensed species (Ti(c), TiN(c)). Thermodynamic properties of the cited species except Ar⁺, N⁺ and TiN(g), are found in JANAF tables [9]. The properties of TiN(g) were evaluated up to 6000 K with theoretical and experimental data by Carlson *et al.* [10] and Stearns and Kohl [11], and the equilibrium constants for the reaction in the system, except Ar=Ar⁺+e⁻, and N=N⁺+e⁻, can be evaluated. For the last two cases, the Saha-Eggert equation was used directly to evaluate the constant [12].

The computational results are shown in Fig. 1, which is based on our experimental conditions: Ar=40 litre min⁻¹, N₂=1 litre min⁻¹ and Ti=0.3 g min⁻¹ (see Table I.) The total pressure of the gas phase was assumed to be 1 atm, and the total moles of the mixture is different at each temperature. Such a prediction was adopted for the benefit of the enthalpic considerations. Under the assumed conditions, Ti(c) cannot be present. This means that such a low flow rate of nitrogen is sufficient to produce the TiN particles from the gas mixture. The condensation temperature of TiN(c) is 2760 K, which shows that the solid particle of TiN may grow from the vapour phase directly, because the melting temperature is about 3220 K. Moreover, the mole concentrations of N, Ti⁺, e⁻ and TiN(g) are in the same order at the condensation temperature. These species may play important roles as nucleus centres at the beginning of a homogeneous nucleation. When the TiN(s) is condensed from the vapour phase, 1 kcal min⁻¹

is generated. Therefore, an appropriate heat sink is needed if one wishes this reaction to proceed rapidly. The power needed to raise the temperature of 40 litre min⁻¹ argon gas up to 6000 K is about 52.6 kcal min⁻¹, which may be regarded as enthalpy in the exit gas from the torch. However, when 1 litre min⁻¹ nitrogen and 0.3 g min⁻¹ titanium are added to the argon, a power of about 63 kcal min⁻¹ is needed. According to a heat balance of an r.f. plasma investigated by Miller and Ayen [13], the values reveal that an increase in power of about 6.7 kW at plate power level is needed to stabilize the plasma; otherwise the temperature of the plasma would be lowered and quenched. These considerations are based on the assumptions that the thermodynamic equilibrium is retained in the plasma tail flame and all of the feed materials are to be heated to the plasma temperature. The calculated equilibrium diagram may not be strictly applicable to the plasma tail flame. However, such a diagram may contribute to a better understanding of the complex phenomena in the plasma tail flame.

3. Experimental details

3.1 Materials

The feed titanium powder was supplied by Toho Titanium Co., with specification of 99.1%. The maximum size of a particle which can be vaporized completely in the r.f. plasma was estimated from our model [14], and determined by the preliminary experiments. The powder was then sieved to

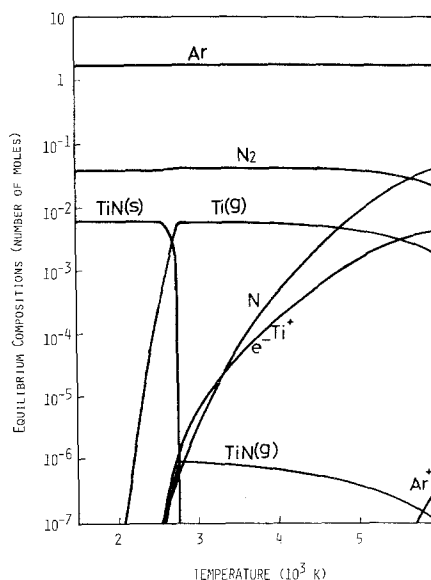


Figure 1 Thermodynamic equilibrium diagram for the Ar–Ti–N system.

a size less than $25\ \mu\text{m}$, and dried in a vacuum chamber at 100°C for 5 h to improve the fluidity. Argon and nitrogen gases were supplied by Toyo Sanso Co, with specifications of 99.998%. No refinement was done.

3.2. Apparatus and procedure

The experimental apparatus consists of an r.f. generator (nominal maximum output was 30 kW and the frequency was approximately 4.0 MHz), a plasma reactor, a powder feeder, gas supply system, water-cooling system, and an exhaust system. The reactor chamber designed for this study is schematically shown in Fig. 2. The reactor, in which the plasma is discharged and the product is collected, consists of three major components: a stainless steel outer jacket (30 cm diameter \times 64 cm), a water-cooled Pyrex cylinder for the collection of the products, and a torch. The torch was similar to the one developed by Reed [15]. Basically it consists of a work coil and three concentric quartz tubes with three independent gas flows: outer, inner and carrier gas flows. Nitrogen was added to the outer flow, and the titanium powder was fed into the plasma by the carrier gas through the centre tube. The outer tube was cut just below the work coil to prevent

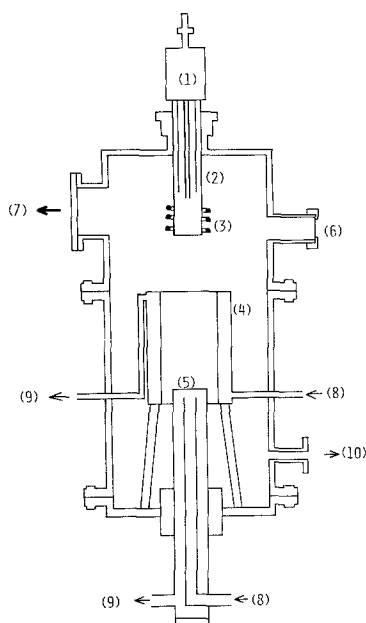


Figure 2 Reactor chamber designed for powder processing studies. (1) Torch head, (2) three concentric quartz tubes, (3) work coil, (4) water-cooled Pyrex cylinder, (5) water-cooled copper quenching plate, (6) window, (7) to generator, (8) water in, (9) water out, (10) to exhaust system.

the wall melting and products being deposited on the torch. The work coil used was made of a two-plus-one turn helical quartz tube (10 mm diameter) into which a braided copper wire was threaded, which was the same as that designed by Giovanelli [16]. This was useful in preventing a discharge between the coil and the chamber or the plasma flame. Operating conditions are shown in Table I.

More than 90% of the products were deposited on the inner surface of the water-cooled Pyrex cylinder. To collect the product samples suitable for an electron microscopy, microscope grids (standard electron microscope 200-mesh copper grids (3 mm diameter) carrying Formbar or Colloidion film coated with evaporated carbon) were pressed lightly on to the surface and were then examined. The products were also scraped together with a brush from the surface, and were used for the X-ray diffraction and chemical analysis.

4 Results and discussion

4.1. Chemical analysis

Each sample was weighed and slowly heated ($10^\circ\text{C min}^{-1}$) up to 1300°C in a platinum crucible in an oxygen flow, and heating was continued at this temperature until a constant weight was achieved. From the weight of the white TiO_2 produced, the titanium content of the sample was determined. For nitrogen content, Kjeldahl N-determinations method was first adopted, but the products did not dissolve completely in boiling acid after 12 h, therefore the nitrogen content was determined as follows. A small amount of the product (about 5 mg) was mixed with 0.5 g standard nickel powder whose nitrogen content had been already analysed. The total nitrogen content of the mixed sample was determined using a LECO analyser. The true nitrogen content of the product was then estimated from the difference. The high surface area of the product makes it difficult to determine

TABLE I Operating conditions

1. Gas flow rate
Inner Ar = 8 litre min^{-1}
Outer Ar = 30 litre min^{-1}
Outer N_2 * = 0.5 ~ 2.0 litre min^{-1}
Powder carrier Ar = 2.0 litre min^{-1}
2. Plate power output = 7.5 [kV] \times 4.1 [A]
3. Powder feed rate* = 0.022 ~ 0.31 g min^{-1}

*Variable.

the oxygen content precisely. The residue was assigned as oxygen impurity in this study.

Fig. 3 shows the results of the chemical analysis. The chemical compositions of the products are plotted as functions of the reactant composition, i.e. the nitrogen to titanium molar ratio. It was found that the titanium content gradually decreased over the range of experimental conditions investigated. The nitrogen content was almost independent of molar ratio for $[N_2]/[Ti] > 10$. On the other hand, the oxygen content as an impurity increased to a considerable degree. The chemical formulae of the products which appear in Fig. 3 are shown in Table II. Obviously, these results are characterized by the higher oxygen contents, especially in the case of the higher $[N_2]/[Ti]$ molar ratio. It is well known that the ultrafine particle surface is oxidized more or less while being handled in air. However, such a high content of oxygen is not well explained merely by the air oxidation mechanism. As shown in Table I, the main variable in this experiment was the powder feed rate, and the oxygen content was re-plotted as a function of this (Fig. 4). In the same figure, the theoretical curve was drawn from the assumptions that the purity of argon and nitrogen was 99.99%, which contained 0.01% oxygen as an impurity, i.e. the partial pressure of oxygen in the chamber was 10^{-4} atm, and that the feed titanium reacted with all the oxygen contained in the flowing gases, before reacting with the nitrogen completely. This good agreement between theoretical and experimental values shows that the main reason for such a high oxygen content in the product is not attributable

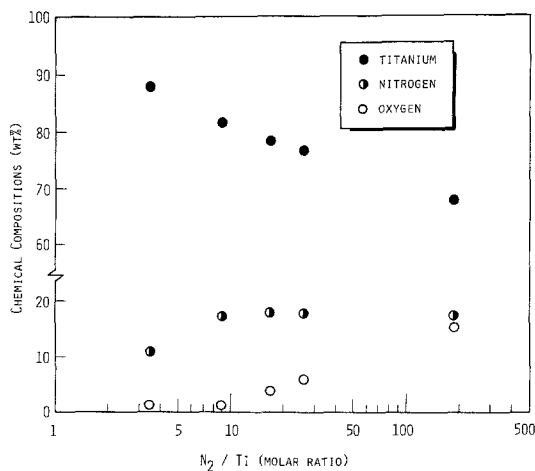


Figure 3 Effect of $[N_2]/[Ti]$ molar ratio on the chemical compositions.

TABLE II Chemical compositions

Sample	$[N_2]/[Ti]$ (molar ratio)	Chemical compositions	
		Formula 1	Formula 2
A	3.5	TiN _{0.43} O _{0.05}	Ti(NO) _{0.48}
B	9	TiN _{0.73} O _{0.04}	Ti(NO) _{0.77}
C	17	TiN _{0.78} O _{0.14}	Ti(NO) _{0.92}
D	26	TiN _{0.79} O _{0.22}	Ti(NO) _{1.01}
E	190	TiN _{0.88} O _{0.67}	Ti(NO) _{1.55}

to the high specific surface area of the products; but to the purity of the flowing gases. As a result, two methods to minimize the oxygen content in the product can be proposed. The first is to purify the gases and keep the oxygen partial pressure in the chamber less than 10^{-6} atm, although it is very difficult and expensive to purify such high flow-rate gases. The second, which is more realistic, is to adopt a higher feeding rate of titanium, at least 1 g min^{-1} . This method requires a higher power r.f. generator than the one used in this experiment, because it also requires a higher flow rate of nitrogen. From Table II, one can estimate that about $10 \text{ litre min}^{-1}$ nitrogen must be added to the outer flow in order to prepare stoichiometric titanium nitride. In conclusion, it may safely be said that the high oxygen content is not an attribute of the particles prepared by an r.f. plasma process, but depends to a large extent upon experimental conditions.

4.2. X-ray diffraction

The line profiles were recorded at room temperature by chart, using a Rigaku Denki diffractometer with Ni-filtered $\text{CuK}\alpha$ radiation. The centre of gravity of each line was measured and the corresponding value of the lattice parameter was calculated and plotted against the Nelson-Riley function. The extrapolation to 90° in θ was made

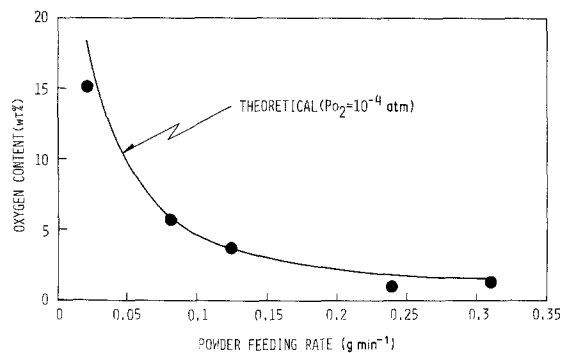


Figure 4 Effect of powder feeding rate on oxygen content.

by least squares analysis. For all samples, it was possible to observe ten diffraction lines of δ -phase TiN for Bragg angles between 30° and 150° in 2θ . For samples A and B in Table II, one or two weak lines of another phase were also observed, only near 40° in 2θ . This is assumed to be an α -phase of titanium which may be slightly nitrated, but it was impossible to determine the corresponding phase from the lines precisely.

Fig. 5 shows the variation of lattice parameter of the δ -phase with $[N_2]/[Ti]$ molar ratio. It is well-known that the lattice parameter of TiN_x increases linearly and decreases for $x < 1$ and $x > 1$, respectively, and the stoichiometric TiN has a maximum value. Fig. 5 also shows the same tendency, and the lattice parameter of sample D (4.245 Å) agreed well with that of the stoichiometric TiN reported in the literature [17]. The upper limit of x (in TiN_x) previously reported in the literature, is about 1.3 [18]. If the value is adopted, the chemical formula of sample E may be written as $0.6(TiN_{1.3}) \cdot 0.4(TiO_{1.9})$. However, the results of X-ray (and electron) diffraction analysis showed no existence of TiO_2 , but δ -phase only, and it can be considered that the oxygen in the products dissolve into the δ -phase completely. So, if oxygen-free product are to be prepared in future, the product with $x \geq 1.3$ must be prepared for the experimental conditions of sample E. These results show that it is possible to control the composition in the product and there appears to be an optimum molar ratio of $[N_2]/[Ti]$ for making a stoichiometric TiN by an r.f. plasma process: namely, $[N_2]/[Ti] = 26$ under these experimental conditions.

4.3. Electron microscopy

The particles collected on the microscope grids were observed with a JEM-7A electron microscope

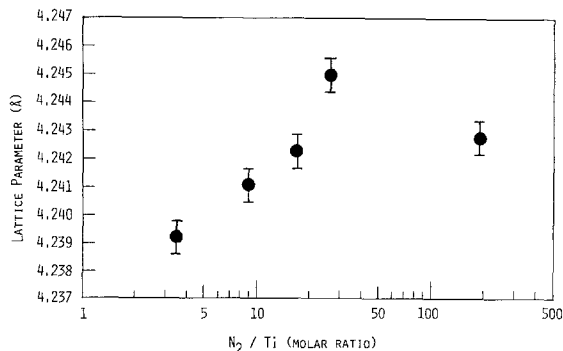


Figure 5 Variation of lattice parameter with $[N_2]/[Ti]$ molar ratio.

operated at 150 kV. A liquid-nitrogen trap placed just above the specimen was used to reduce the rate of contamination of the particles in the electron microscope. Over 50 specimens were observed and about 300 pictures were taken at various magnifications from 10 000 to 130 000 on the fluorescent screen.

From examination of the electron micrographs of various samples, it was found that a higher feed rate of titanium powder resulted in a larger particle size, although the difference was very small, as shown in Fig. 6. It was also found that the majority of the particles with diameters larger than 20 nm showed clear-cut habits (Fig. 7), and no significant difference in the shapes was found amongst the samples. (The shapes of particles with diameters less than 10 nm were not identified because of the resolution limit.) Moreover, electron diffraction patterns of all samples showed only the NaCl-type structure, i.e. δ -phase of TiN, and traces of titanium oxides such as Ti_2O_3 and TiO_2 were not found. These results are consistent with the results of X-ray diffraction analysis.

The shapes of the particles can be classified in three groups: cube (A), tetrahedron (B) and rhombic dodecahedron (C) (Fig. 8). Most of the crystallites belonged to type A, while the other

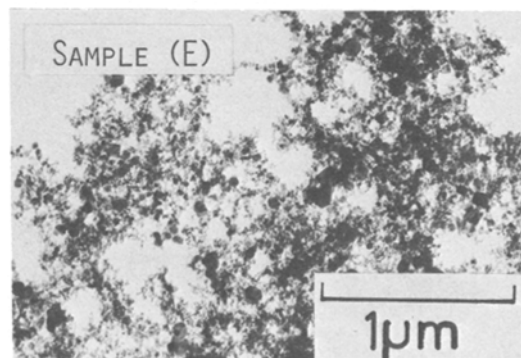
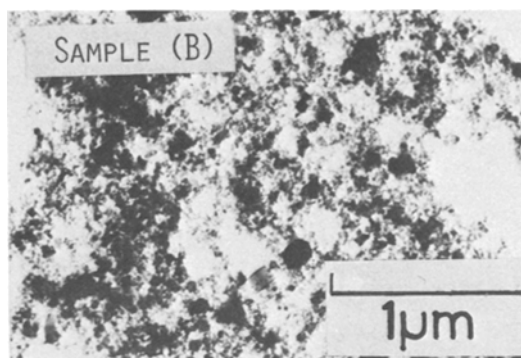


Figure 6 Electron micrographs of samples B and E.

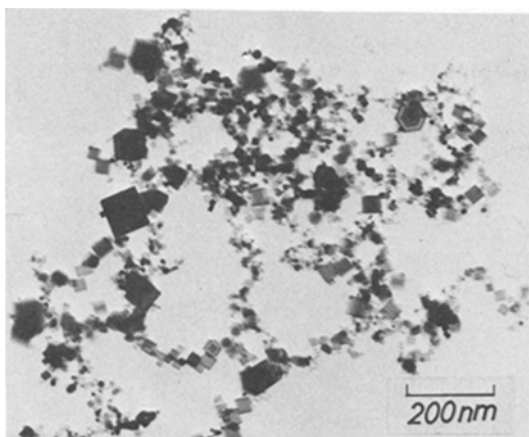


Figure 7 Electron micrograph of particles with clear-cut habits (sample C).

two types were less than a few percent. The profile of the particles and the geometric arrangement of equal-thickness fringes suggest that particles A, B, and C are bounded by six (100)-planes, four (111)-planes and twelve (110)-planes, respectively. It is well-known that these three planes are equilibrium-form faces of a simple cubic mixed crystal [19]. The equilibrium form is governed by the anisotropy of the surface energy. The NaCl-type structure (δ -phase of TiN) can be also considered as an ordered simple cubic mixed crystal. Therefore, the surface energy for the (100) face of TiN is lower than the other two faces, which means that the preferential growth form is a cube bounded by (100)-planes. These results show that each particle is a single crystal of TiN and may effectively resist the oxygen in the air because of the dense and clean surface appearance, which is supported by the fact that the ultrafine particles resisted the acid strongly as mentioned in Section 4.1. At this stage, it is inexplicable why these three kinds of particles were grown simultaneously; however, the same results were reported recently by Nickl *et al.* [20] who investigated the preferential growth form of TiN single crystals which were deposited from the $\text{TiCl}_4\text{-N}_2\text{-H}_2$ system at 1800 K on to a polycrystalline TiN substrate. They found that the preferential growth form was a cube bounded by (100)-planes. (111)-, (110)- and (113)-planes were also found in their investigations.

It was sometimes observed that the golden-yellow coatings of TiN were formed on the surface of the copper quenching plate in Fig. 2. This means that the water-cooled Pyrex cylinder is



Figure 8 Three typical types of ultrafine TiN particles found in this study.

filled with high-temperature titanium vapour, and the growth of the particles was restricted in the vicinity of the inner surface of the cylinder where a steep temperature gradient exists. If more effective quenching devices are developed, finer and more uniform size particles could be prepared.

5. Conclusions

A reactor chamber was designed for powder processing studies by r.f. plasmas. Using the reactor, ultrafine titanium nitride with a statistical median size of about 10 nm, was prepared starting from 25 μm titanium powder and nitrogen as the nitriding agent. The conversion efficiency was close to 100%. The thermodynamics of the process were considered and contributed towards a better understanding of the process.

The following conclusions can be made.

- (1) The $[\text{N}_2]/[\text{Ti}]$ molar ratio affects the composition of the products but has little effect on the shape of the particles.
- (2) It is possible to control the composition of the products and there appears to be an optimum molar ratio of $[\text{N}_2]/[\text{Ti}]$ for making stoichiometric TiN.
- (3) Each particle is a single crystal and the preferential growth form is a cube bounded by (100)-planes.
- (4) The high oxygen content in the products is not an attribute of the particles prepared by an r.f. plasma process, but depends to a large extent upon experimental conditions.
- (5) The experimental studies are in an early stage, but provide evidence to suggest that new materials can be produced by an r.f. plasma process, in particular the ultrafine refractory nitrides.

Acknowledgements

The authors wish to thank Professor H. Nagai (Osaka University) for chemical analysis with

LECO analyser and Daido Steel Co, Ltd for making the chamber. Financial support by the Ministry of Education of Japan is also gratefully acknowledged.

References

1. R. M. POWELL, W. STOCPOŁ and M. TINKHAM, *J. Appl. Phys.* **48** (1977) 788.
2. A. SCHNEIDER, R. GEHRKE, M. KRETSCHMER and M. WASSERMANN, *Metall.* **23** (1969) 230.
3. J. HOJO, O. IWAMOTO, Y. MARUYAMA and A. KATO, *J. Less-Common Metals* **53** (1977) 265.
4. B. WALDIE, *Chem. Eng.* **259** (1972) 92.
5. R. MAHE, "Les Hautes Températures et leurs Utilisations en Physique et en Chimie", Vol. 1, edited by G. Chaudron and F. Trombe (Masson and Cie., Paris, 1973) p. 139.
6. V. N. TROITSKII, B.M. GREBTSOV and M. I. AIVAZOV, *Sov. Powder Met. Metal Ceram.* **12** (1974) 869.
7. I. M. MACKINNON and B. G. REUBEN, *J. Electrochem. Soc.* **122** (1975) 806.
8. J. CANTELOUP and A. MOCELLIN, "Special Ceramics 6", edited by P. Popper (B. Ceram. R.A., Stoke-on-Trent, 1975) p. 209.
9. JANAF Thermochemical Tables (Dow Chemical Company, Midland Michigan, 1970).
10. K. D. CARLSON, C. R. CLAYDON and C. MOSER, *J. Chem. Phys.* **46** (1967) 4963.
11. C. A. STEARNS and F. J. KOHL, *High Temp. Sci.* **2** (1970) 146.
12. W. H. DRAWIN and P. FELENBOK, "Data for plasmas in local thermodynamic equilibrium" (Ganthier-Villars, Paris, 1965).
13. R. C. MILLER and R. J. AYEN, *J. Appl. Phys.* **40** (1969) 5260.
14. T. YOSHIDA and K. AKASHI, *ibid* **48** (1977) 2252.
15. T. B. REED, *ibid* **32** (1961) 821.
16. R. GIOVANELLI, *ibid* **41** (1970) 3194.
17. W. B. PEARSON, (ED), "Handbook of lattice spacings and structures of metals", Vol. 2 (Pergamon, London, 1967) p. 455.
18. A. N. CHRISTENSEN, *Acta Chem. Scand.* **A29** (1975) 563.
19. R. LACMANN and G. M. POUND, *Z. Phys. Chem. (N.F.)* **53** (1967) 143.
20. J. J. NICKL, K. SCHWEITZER and A. HAHLEWEG, *J. Less-Common Metals* **51** (1977) 235.

Received 8 August and accepted 16 November 1978.